PAPER • **OPEN ACCESS**

Measurement of the strengths of the resonances at 417, 458, 611, 632 and 1222 keV in the $^{22}Ne(p,\gamma)^{23}Na$ reaction

To cite this article: Federico Ferraro 2018 *J. Phys.: Conf. Ser.* **940** 012041

View the article online for updates and enhancements.

You may also like

- A depth-encoding PET detector that uses light sharing and single-ended readout with silicon photomultipliers
Zhonghua Kuang, Qian Yang, Xiaohui Wang et al.

- SPECTRAL STATE DEPENDENCE OF THE 0.4–2 MEV POLARIZED EMISSION IN CYGNUS X-1 SEEN WITH *INTEGRAL*/IBIS, AND LINKS WITH THE AMI RADIO DATA
Jérôme Rodriguez, Victoria Grinberg, Philippe Laurent et al.

- Perpendicularly magnetized ferromagnetism in Mn/Al bilayer thin films on Si substrates induced by temperature dependent ion beam mixing
H Khanduri, S A Khan, Mukesh C Dimri et al.

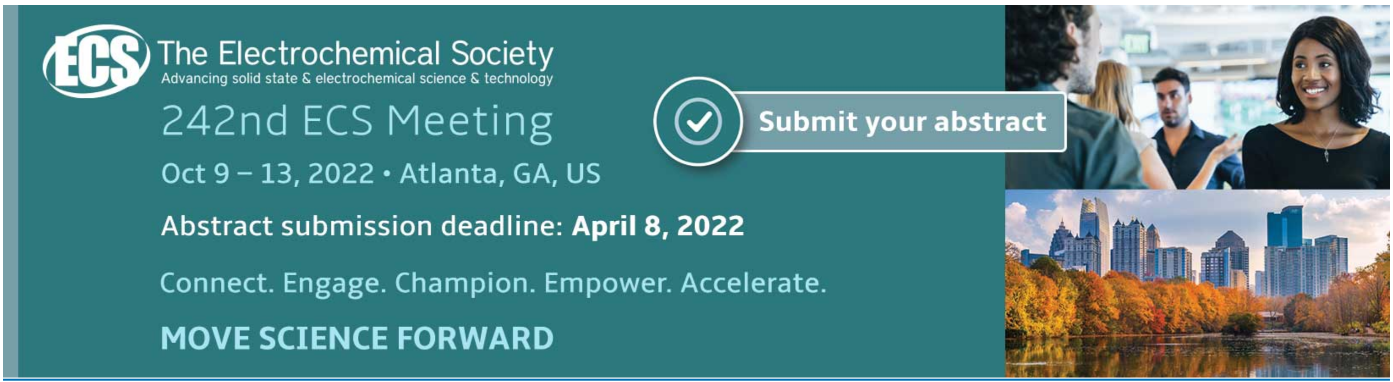

This content was downloaded from IP address 159.149.193.175 on 02/03/2022 at 11:09

Measurement of the strengths of the resonances at 417, 458, 611, 632 and 1222 keV in the $^{22}\mathrm{Ne(p,\gamma)}^{23}\mathrm{Na}$ reaction

Federico Ferraro

Dipartimento di Fisica, Università degli Studi di Genova and INFN, Sezione di Genova
Via Dodecaneso 33, 16146 Genova, Italy

E-mail: `federico.ferraro@ge.infn.it`

Abstract. The $^{22}\mathrm{Ne(p,\gamma)}^{23}\mathrm{Na}$ reaction is part of the NeNa cycle of hydrogen burning. This cycle plays a key role in the nucleosynthesis of the elements between ^{20}Ne and ^{27}Al in red giant stars, asymptotic giant stars and classical nova explosions. The strengths of the resonances at proton energies above 400 keV are still affected by high uncertainty. In order to reduce this uncertainty, a precision study of some of the most intense resonances between 400 keV and 1250 keV has been performed at the HZDR 3 MV Tandetron. The target, made of ^{22}Ne implanted in a 0.22 mm thick Ta backing, has been characterized using the 1222 keV and 458 keV resonances, well known in literature. Subsequently, the strengths of the resonances at 417, 458, 611, 632 and 1222 keV were determined. Two HPGe detectors equipped with active anti-Compton shielding have been used.

1. The $^{22}\mathrm{Ne(p,\gamma)}^{23}\mathrm{Na}$ reaction and the NeNa cycle of hydrogen burning.

The $^{22}\mathrm{Ne(p,\gamma)}^{23}\mathrm{Na}$ reaction is part of the NeNa cycle of hydrogen burning (see Figure 1), active in red giant branch (RGB) stars, asymptotic giant branch (AGB) stars, classical novae (CN) and supernovae Ia (SN Ia) explosions. This cycle greatly influences the nucleosynthesis of the elements between ^{20}Ne and ^{27}Al because of its link to the MgAl cycle [1, 2]. At temperatures of about 0.4 GK (for CN) up to 1.5 GK (for SN Ia) and above, the greatest contribution to the reaction rate comes from the resonances between 400 keV and 1250 keV (see Figure 2), some of which are affected by high uncertainty [3]. Because of the lack of knowledge on some of these resonances, the $^{22}\mathrm{Ne(p,\gamma)}^{23}\mathrm{Na}$ reaction rate is very uncertain, asking for a deeper investigation of the existing resonances and a better determination of their strengths [4].

2. Experiment

The measurements have been performed at the 3 MV Tandetron accelerator of Helmholtz-Zentrum Dresden-Rossendorf in Dresden, Germany. A solid target has been used, made of ^{22}Ne implanted on a 0.22 mm thick Ta backing. The typical proton current provided by the accelerator was 10 μA. The target was water-cooled and a copper tube in front of the target (see Figure 3 for a section drawing of the setup), connected to a voltage of -100 V, provided the secondary electrons suppression, so that the collected charge has been measured at 1% uncertainty.
Two high purity germanium (HPGe) detectors equipped with BGO active shielding and

Content from this work may be used under the terms of the Creative Commons Attribution 3.0 licence. Any further distribution of this work must maintain attribution to the author(s) and the title of the work, journal citation and DOI.
Published under licence by IOP Publishing Ltd

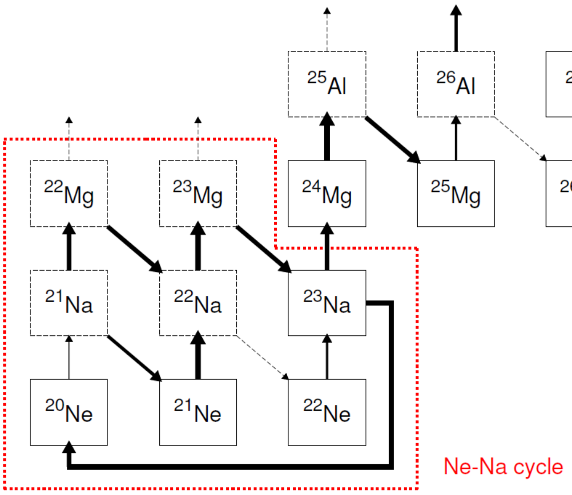

Figure 1. The NeNa cycle and its link to the MgAl cycle.

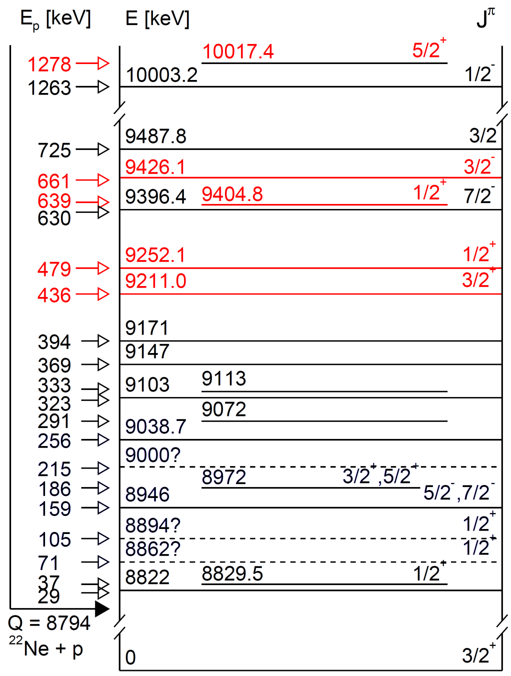

Figure 2. ^{23}Na excited states. In red the measured resonances (E_p in the laboratory frame of reference).

surrounded by lead have been positioned at 55° and 90° (see Figure 4 for a picture of the setup). A lead collimator has been put in front of each detector in order to shield the BGO and better define the solid angle for the HPGe detectors. The active BGO shielding, together with the anti-coincidence trigger, provided a background reduction by a factor of 3 without any significant reduction of the peak efficiency.
The yield curve of the well known narrow resonance at 1222 keV permitted to monitor the target stability over time and to measure the implantation profile. The energy and efficiency calibrations have been carried out owing to some standard radioactive sources (^{137}Cs, ^{60}Co and ^{88}Y) together with the well known reaction ^{27}Al(p, γ)^{28}Si, which permitted the extension of the range of these measurements up to 10763 keV. A target scan has been done for each resonance and the yield curve has been studied. A long run has been acquired on the top of each resonance yield curve to determine the resonance strength.

3. Analysis

The ^{23}Na characteristic peaks have been recognized in the spectra and the Ta/^{22}Ne ratio has been determined normalizing our results to the 1222 keV and 458 keV resonance strengths, thus improving the determination of the stoichiometry, which turned out to be Ta/^{22}Ne $= 7.92 \pm 0.04_{\rm stat} \pm 0.34_{\rm syst} \pm 0.56_{\omega\gamma}$ as shown in [7].
The primary transition peaks have been clearly identified for each resonance and the background subtraction has been done. The total yield has been calculated using

$$Y_{tot} = \frac{e}{Q} \sum_i \frac{N_{\gamma_i}}{W_{\gamma_i} \eta_{\gamma_i}} \tag{1}$$

where $\frac{e}{Q}$ is the reciprocal of the total number of incident particles, N_{γ_i}, W_{γ_i} and η_{γ_i} are respectively the number of counts, the angular correlation coefficient [6, 7] and the efficiency of

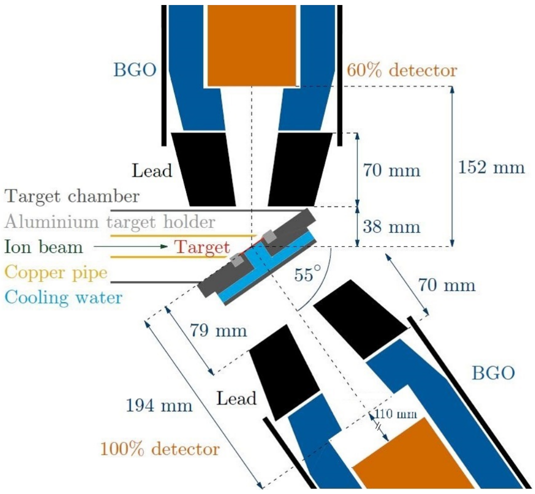

Figure 3. Setup drawing. BGO detectors are used as anti-Compton veto.

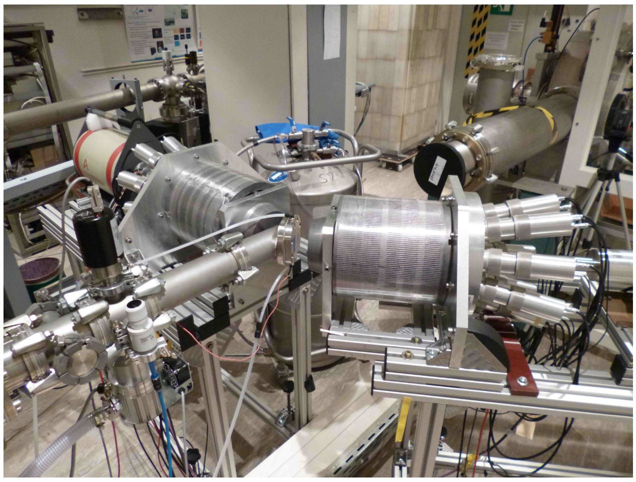

Figure 4. Setup picture. On the left side the target chamber is visible.

the i^{th} primary transition photon. The stopping power in ^{22}Ne and Ta has been evaluated with SRIM and the resonance strengths were determined using the equation

$$Y_{max} = \frac{\lambda^2}{2}\omega\gamma\frac{M+m}{M}\frac{1}{\epsilon} \tag{2}$$

where λ is the De Broglie wavelength, $\omega\gamma$ is the resonance strength, M and m are respectively the masses of the target nucleus and the projectile and ϵ is the effective stopping power in the Ta - ^{22}Ne compound.

4. Results

In conclusion, we measured ^{22}Ne$(\mathrm{p},\gamma)^{23}$Na resonance strengths for E_{CM}=417, 458, 611, 632, 1222 keV. The obtained strengths and their impact on the reaction rate are reported in [7], together with a more complete description of the experiment.
These measurements are complementary to the resonance strengths measured by LUNA at lower energies [4, 8, 10] and will improve our knowledge of the thermonuclear reaction rate.

Acknowledgments

This work has been supported by the European Union (SPIRIT EC contract no. 227012) and by NAVI (HGF VH-VI-417).

References

[1] Marion J and Fowler W 1957 *Astrophys. J.* **125** 221-32
[2] Iliadis C, Champagne A, José J, Starrfield S and Tupper P 2002 *Astrophys. J. Suppl. Ser.* **142** 105-37
[3] Iliadis C, Longland R, Champagne A E and Coc A 2010 *Nuclear Physics* A **841** 251-322
[4] Cavanna F *et al.* 2014 *Eur. Phys. J.* A **50** 179
[5] Longland R *et al.* 2010 *Phys. Rev.* C **81** 055804
[6] Viitasalo M, Piiparinen M and Anttila A 1972 *Z. Physik* **250** 387-394
[7] Depalo R *et al.* 2015 *Phys. Rev.* C **92** 045807
[8] Cavanna F *et al.* 2015 *Phys. Rev. Lett.* **115** 252501
[9] Ferraro F *et al.* *PoS NIC XIII* 093
[10] Depalo R and Cavanna F *PoS NIC XIII* 087